Colloid Polym Sci (2007) 285:1581–1591
DOI 10.1007/s00396-007-1729-2

ORIGINAL CONTRIBUTION

High compact melamine-formaldehyde microPCMs containing *n*-octadecane fabricated by a two-step coacervation method

Jun-Feng Su · Zhen Huang · Li Ren

Received: 21 March 2007 / Revised: 19 June 2007 / Accepted: 22 June 2007 / Published online: 19 July 2007

Abstract Microcapsules containing *n*-octadecane were successfully fabricated by an in-situ polymerization process with melamine-formaldehyde (MF) prepolymer and a hydrolyzed copolymer of styrene and maleic anhydride (SMA) as shell materials. To achieve a long service time of microcapsules containing phase change materials (microPCMs), the compactness of shells was improved by adding the MF prepolymer twice. The mechanism of this method was a two-step coacervation (TSC) under the help of hydrolyzed SMA compared to a one-step coacervation (OSC). To understand the influence of both coacervations, properties of shells were investigated in terms of morphologies, density, thickness, and stability by means of scanning electron microscopy (SEM), transmission electron microscopy, and thermal gravimetric analysis (TGA). The data of shells thickness were achieved from the cross-section SEM images. It shows that the average thickness of shells from two kinds of process are 0.1 μm. The density and stability in water of shells fabricated by TSC are both higher than that of shells by OSC. TGA curves show the expected microPCMs of TSC losing weight from 200 to 400 °C. The release curves, relationship between time and logarithmic residual weight of core, show there are two decrease-linear steps after curve regression. It can be concluded from all these results that the TSC method may be a promising method leading to a compact shell structure for various application.

Keywords Microcapsules · MicroPCMs · Coacervation · Compact · Melamine-formaldehyde resin

J.-F. Su (✉) · Z. Huang
Institute of Chemistry and Materials,
Tianjin University of Commerce,
Tianjin 300134, People's Republic of China
e-mail: sujunfeng2000@yahoo.com.cn

L. Ren
Polymer Research Institute,
College of Chemical Engineering and Technology,
Hebei University of Technology,
Tianjin 300130, People's Republic of China

Introduction

In recent years, phase change materials (PCMs) have attracted ever-increasing attention because they can absorb or release large latent heat at their melting points as surrounding temperature increases or decreases. Thus, they could be potentially used in active or pumped coolants, solar and nuclear heat storage systems, and heat exchangers [1]. Although very high latent heat can be obtained, the bulk PCMs are not easy to handle in practical application [2]. The recent advances of microcapsules containing PCMs (microPCMs) have provided an interesting alternative for using PCMs in the manufacture of thermoregulated fibers, fabrics, foams, and building materials [3–8]. In these studies, a series of microPCMs were fabricated and properties, including diameter, surface morphology, melting or crystallization, and thermal stability, were investigated by means of Fourier transform infrared spectroscopy, scanning electron microscopy (SEM), differential scanning calorimetry, thermal gravimetric analysis (TGA) and differential thermal analysis [9–12]. Melamine-formaldehyde (MF) resin [9, 10], urea-formaldehyde resin [11, 12], and polyurethane [13–15] were usually selected as shell materials of microcapsule for the PCMs protection. In practical usages of microPCMs, the volume of PCM in shells will change obviously during absorbing and releasing thermal energy. The volume alternant changes originally bring the liquefied PCMs leaking from the microcapsules.

And the breakage of the shell will happen based on the mismatch of thermal expansion of the core and shell materials at high temperature [13]. Therefore, it is necessary to keep the shell stability and compact for a long-life with less cracks and lower permeability.

MF resin has been successfully applied as shell material of microcapsules in fields of carbonless copying paper, functional textiles, liquid crystals, adhesives, insecticides, and cosmetics [16]. Furthermore, literatures have shown that MF has been applied for microPCMs encapsulating various solid–liquid PCMs with the size range of about 50 nm to 2 mm. Generally, MF resin is adsorbed and cured on surfaces of core particles though an in situ polymerization with the help of a polymeric surfactant. Although MF resin is widespread as shell material, our knowledge about the physical properties of these shells has developed very slowly. As the polymic shell is a thin membrane covering on a particle, it is very difficult to confirm its properties. However, it is very essential to know the density, thickness, and stability of shells, which directly affect the permeability, mechanical strength, and service time of microcapsules.

In addition, literatures have reported the relationship between the shell morphologies and permeability [17–20]. In these previous researches the mechanism of controlling permeability is to decrease the shell defects, such as methods of adding accessory ingredients, modeling the degree of cross-linking, and changing the molecular structure of shell polymer. Also, several new techniques for compact encapsulation have been developed, such as increasing the molecular weight of polymer, the expansion ability, and the mechanical strength [21–23].

Besides all the above-mentioned technologies, MF shells are all fabricated by in situ polymerization with a process of one-step dropping monomers for suitable thickness and structure of shells. The mechanism of one-step dropping monomers means a one-step coacervation (OSC) of prepolymer [24–32]. These microcapsules cannot be satisfied with the nonpermeable need of some special core materials such as PCMs, liquid crystal, and biological active materials, which are not expected to be released and contaminated by our environment. Therefore, it is a very important approach to fabricate compact shells and realize the microcapsulation coacervation mechanism of shell.

It is interesting to note that relative to one-step coacervation, the above problem may be successfully solved by a two-step coacervation (TSC) technology, which relies upon a process of adding MF prepolymer twice and leading to TSC on core particles. In this paper, the influence of different coacervations on the properties of microcapsule shells had been investigated.

Experimental

Materials

Styrene–maleic anhydride (SMA) copolymer solid (Scripset® 520, Hercules, USA) was used as a dispersant. A small percentage of the anhydride groups have been established with a low molecular weight alcohol and it is fine, off-white, free flowing power with a faint, aromatic odor. Nonionic surfactant, NP-10 [poly (ethylene glycol) nonylphenyl] from Sigma Chemical, was used as an emulsifier. The prepolymer of MF resin (solid content 50± 2wt%) was purchased from Shanghai Hongqi. Chem. (Shanghai, China). The *n*-octadecane purchased from Tianjin Fine Chemical (Tianjin, China) was encapsulated as the core material. All other chemical reagents were analytical purity and supplied by Tianjin Kermel Chemical Reagent Development Center (Tianjin, China).

Fabrication of TSC microPCMs

Microcapsulation by coacervation proceeds along three main steps:

(1) Phase separation of the coating polymer solution. SMA (10.0 g) and NP-10 (0.2 g) were added to 100 ml water at 50 °C and allowed mix for 20 min. And then a solution of NaOH (10%) was added dropwise adjusting its pH value to 4–5. The above surfactant solution and n-octadecane (32 g) were emulsified mechanically under a vigorous stirring rate of 3,000 rpm for 10 min using a QSL high-speed disperse machine (Shanghai Hongtai Ltd., Shanghai, China).
(2) Adsorption of the coacervation around the core particles. The encapsulation was carried out in a 500 ml three-neck round-bottomed flask equipped with a condensator and a tetrafluoroethylene mechanical stirrer. The above emulsition was transferred in the bottle, which was dipped in steady temperature flume. Half of MF prepolymer (16 g) was added dropwise with a stirring speed of 1,500 rpm. After 1 h, the temperature was increased to 60 °C with a rate of 2 °C/min. Then another half of prepolymer (16 g) was dropped in a bottle at the same dropping rate.
(3) Solidification of the microparticles. Then the temperature was increased to 75 °C. After polymerization for 1 h, the temperature was decreased slowly at a rate of 2 °C/min to atmospheric temperature.

At last, the resultant microcapsules were filtered and washed with pure water and dried in a vacuum oven. In addition, we could control the average diameter of microcapsules by stirring

speed. Also, the OSC microPCMs were fabricated in this work according to the above process by adding the same amount (32 g) of prepolymer shell material in one step.

Characterization

MicroPCMs colloids in emulsion

After polymerization for 1 h, microPCMs were fabricated in emulsion. 1 ml of the above colloidal solution was extracted and spread on a clean glass sheet (1×3 cm). Photographs of the microcapsules retained in emulsion were taken by an optical microscope (MiVnt Image analyze system, China).

SEM morphologies of microPCMs

The microPCMs were dried in a vacuum oven at 40 °C for 24 h. Then the surface morphological structure was examined by means of a XL30 PHILIPS SEM. SEM experiments were performed at 10 kV after carefully coating with gold-palladium without cracking the shells.

Thickness and density of shells

MicroPCMs (5 g) and paraffin (20 g) were blended to form a homogeneous mixture. After the blend was dried at room temperature, it was carefully cut to form a cross-section by an ultramicrotome (RMC MT-7000, USA). Then half-shelled microcapsules were obtained by removing core material and paraffin with alcohol and distilled water. After the pure shell material had been dried at 40 °C for 2 h, it was very interesting that we could achieve the SEM morphologies of the inside of the shells and the shell thickness. The SEM images were analyzed by MiVnt Image analyze system automatically and the thickness of shells was measured by analyzing in a computer system. Each sample was analyzed at least twice and the average value was recorded. As the observed thickness may be not the equatorial thickness, the average value will be larger than recorded data. Also, the diversity of samples may lead the thickness value to a larger value. The density of shell (ρ) was measured by using an MDMDY-300 density machine (Guangdong, China). The mechanism used to test cumulate density of powder following the equation of

$$\rho = \frac{W}{V} \tag{1}$$

where W is the weight of shell and V is the volume of shell. Using a gas displacement technique to measure volume, the density machine completes each sample analyses in less than 5 min.

MicroPCMs stability in water

Ten grams of dried microcapsules was immersed in 100 ml of pure water. A copper net took out several microcapsules from water after a period of time and then the latter were dried at room temperature. The result of compactness was evaluated through observing changes of shell morphologies through a HITACHI H-800 transmission electron microscopy (TEM).

Thermal stability of microPCMs

The thermal stability characterization was performed on a Dupont SDT-2960 TGA analyzer at a scanning rate of 2–5 °C/min in a flow of 40 ml/min nitrogen.

Measurement of permeation

The permeation of microPCMs will be different in various extraction solvents. In this study, ethyl alcohol was applied as a good solvent, which can easily extract the core material of *n*-octadecane. Under the strong effect penetrability of ethyl alcohol molecules, *n*-octadecane molecules will be extracted through the shells. Thus, we can achieve a qualitative analysis by comparing the permeations of different structure microPCMs. To avoid the deposition of microPCMs, a spread method was applied to investigate the permeation.

One milliliter of pure water suspension with the percentage weight of dried microPCMs being 10% was spread homogeneously with a wire bar on a polyethylene terephthalate (PET) film. Poly(vinyl alcohol) played a role as a binder between the PET film and the microcapsules. The film was cut into 1×1 cm squares.

The squire films were soaked in glass vessels containing 30 ml of ethyl alcohol with a density of 0.97 g/ml. The glass vessels were sealed to avoid volatility, with light stirring at a room temperature. The penetration properties of different microcapsules were evaluated by an UV/visible spectrophotometry in ethyl alcohol. From changes of transmittance of light, we got the relationship between the core material penetrating time and the residual weight (wt%) of core material. In this process, the optical density (OD) of the dispersing medium was measured and converted into the concentration of *n*-octadecane using a calibration curve,

$$\text{Residual weight } (\%) = \frac{OD_0 - OD_t}{OD_0} \times 100\% \tag{2}$$

where OD_0 is the OD of all encapsulated core material in ethyl alcohol and OD_t is the OD of encapsulated core material in ethyl alcohol at a point of permeation time (t).

Results and discussion

Mechanism of TSC

Hydrolyzed SMA is a kind of polymeric surfactant that is soluble in water but sufficiently amphiphilic to be adsorbed by surfaces and interfaces, particularly by dispersed solid or liquid phases [31]. In addition, hydrolyzed SMA plays two important roles during the formation of microcapsules: dispersant and anionic polyelectrolyte [32, 33].

Figure 1 illustrates the complex process for forming the TSC microcapsules. Figure 1a depicts the chemical structure of SMA and hydrolysis polymer. As a kind of polymer dispersant, SMA molecules will be hydrolyzed by NaOH and then the −COO group insert and directional arrange on oil droplet surface. In Fig. 1b, hydrophilic groups of carboxyl arrange alternatively along the backbone chains of SMA molecules. When hydrolyzed SMA molecules are adsorbed at the interfaces of oil droplets, it is easy for the molecules to have such directional arrangement with hydrophobic groups oriented into oil droplet and hydrophilic groups out of oil droplet. This kind of molecular arrangement brings results in a relatively strong electron negative field on the surface of oil particles. Anionic polyelectrolyte hydrolyzed SMA has anionic carboxyl groups that can interact with positively charged MF prepolymer below the ζ potential. The MF prepolymer is in affinity with these particles by static. Then, the reaction of microencapsulation took place under acid and heat effect on the surface of oil particles of emulsion, which formed membrane of capsule in such a way. Figure 1c shows the formation process of the TSC by another prepolymer (MF) addition. Under the effect of heat, the second coacervation will be cross-linked to form another part of shells. This method, including twice-addition prepolymer and twice increasing–decreasing temperature courses, lead to expected compact shells.

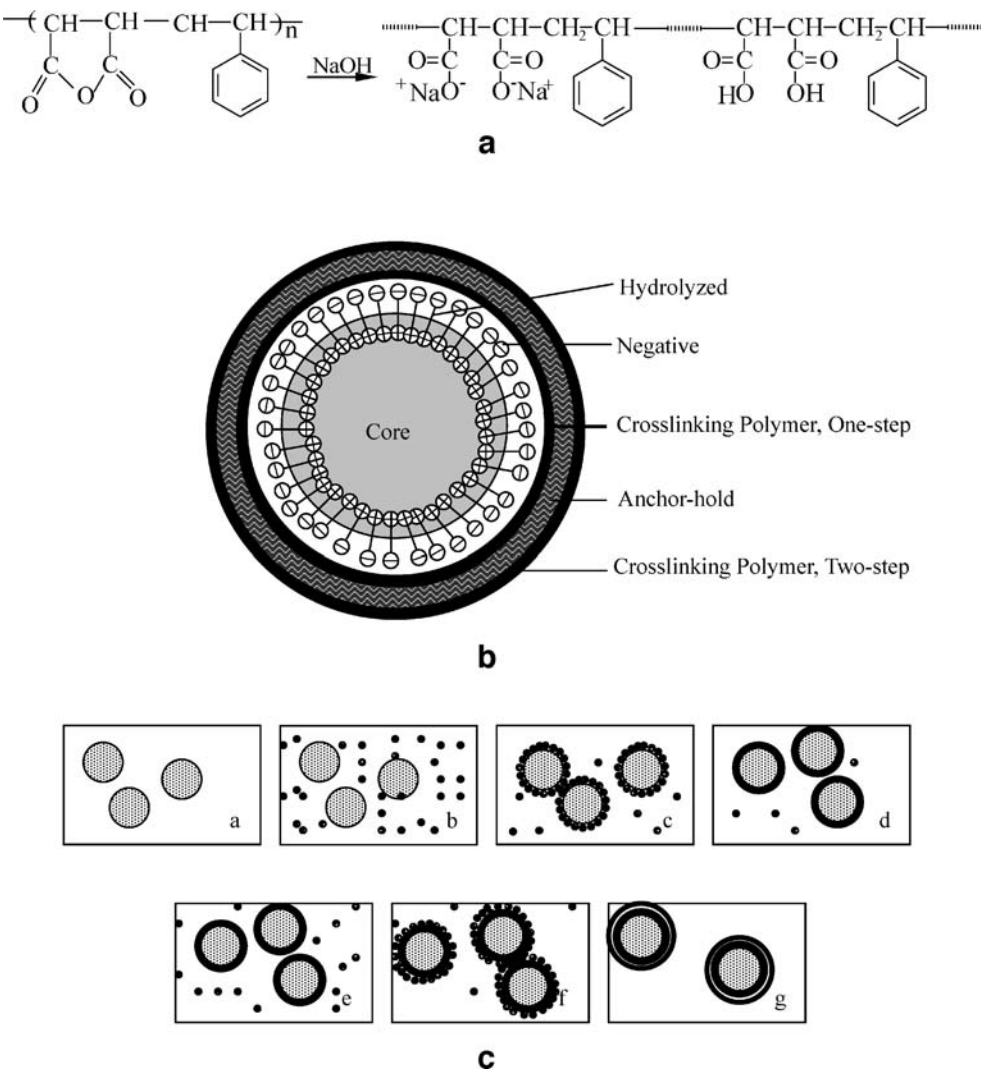

Fig. 1 Sketch mechanism of the fabrication process of TSC microcapsules: **a** chemical structures of SMA alternating copolymer and hydrolysis polymer, **b** the structure of a TSC microcapsule, and **c** the process of fabrication microcapsules by TSC

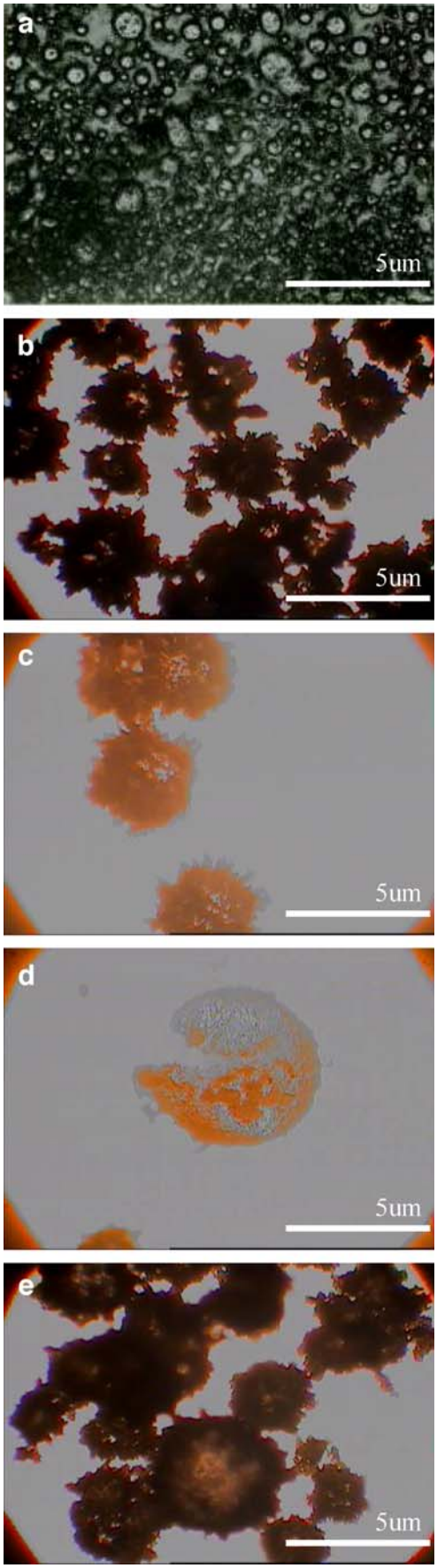

◀ **Fig. 2** Optical microphotographs of microcapsules: **a** core material dispersed by hydrolyzed SMA in water for 5 min, **b** core material dispersed by hydrolyzed SMA in water for 10 min, **c** microcapsules by OSC, **d** a crack OSC microcapsule, and **e** microcapsules by TSC

MicroPCMs in emulsion

To bring the coacervation process to a clear understanding, optical microphotographs of microcapsules were taken to illuminate the details. Figure 2a,b shows morphologies of core material dispersed by hydrolyzed SMA after 5 and 10 min at room temperature. At the beginning of the 5 min, the organic core material was dispersed into particles in water with the help of hydrolyzed SMA molecules. However, these particles had not been separated from each other directly due to the molecule linkage of the hydrolyzed SMA. Being emulsified for 10 min, the core particles were ultimately separated through the regulation of hydrolyzed SMA molecules.

In a previous study [34], we have drawn a conclusion that microPCMs with the average diameter of 1–5 μm, fabricated under stirring speed of 3,000 rpm, is the perfect range of size ensuring both narrow size distribution and enough rigidity. Based on the experiment, MF prepolymer (32 g) was dropped into the above emulsion with a stirring speed of 3,000 rpm. The prepolymer cured on core particles in 60 min by increasing the temperature to 60 °C slowly at a rate of 2 °C/min. Figure 2c shows the optical microphotographs of microcapsules with fleecy or pinpoint morphologies. Imaginably, these incompact structures may lead to cracking or releasing of core material such as the one showed in Fig. 2d.

Compared with OSC microcapsules, Fig. 2e shows the optical microphotograph of TSC ones. The prepolymer covered on particles without cracks and the size distribution of particles is uniform with global and distinct shape. Moreover, there is nearly no conglutination between each microcapsule in very stability solution system.

SEM morphologies of shells

Figure 3a shows SEM morphology of dried OSC microcapsules with the size of 1–5 μm. These microcapsules have a rough morphology and a little polymer occupies the interspaces of microcapsules. It can be contributed to the unencapsulated core material and the uncovered shell material. Especially, the surfaces have many protrusions, which may have occurred by incomplete cross-linking or high-speed chemical reaction. In Fig. 3b–c (×10,000), it is clearly that the surfaces of microcapsules seem to be coarse and porous. It is interesting to note that there is a depressed center on a microcapsule reflecting the lower rigidity of shell in Fig. 3d. We may draw a conclusion from these

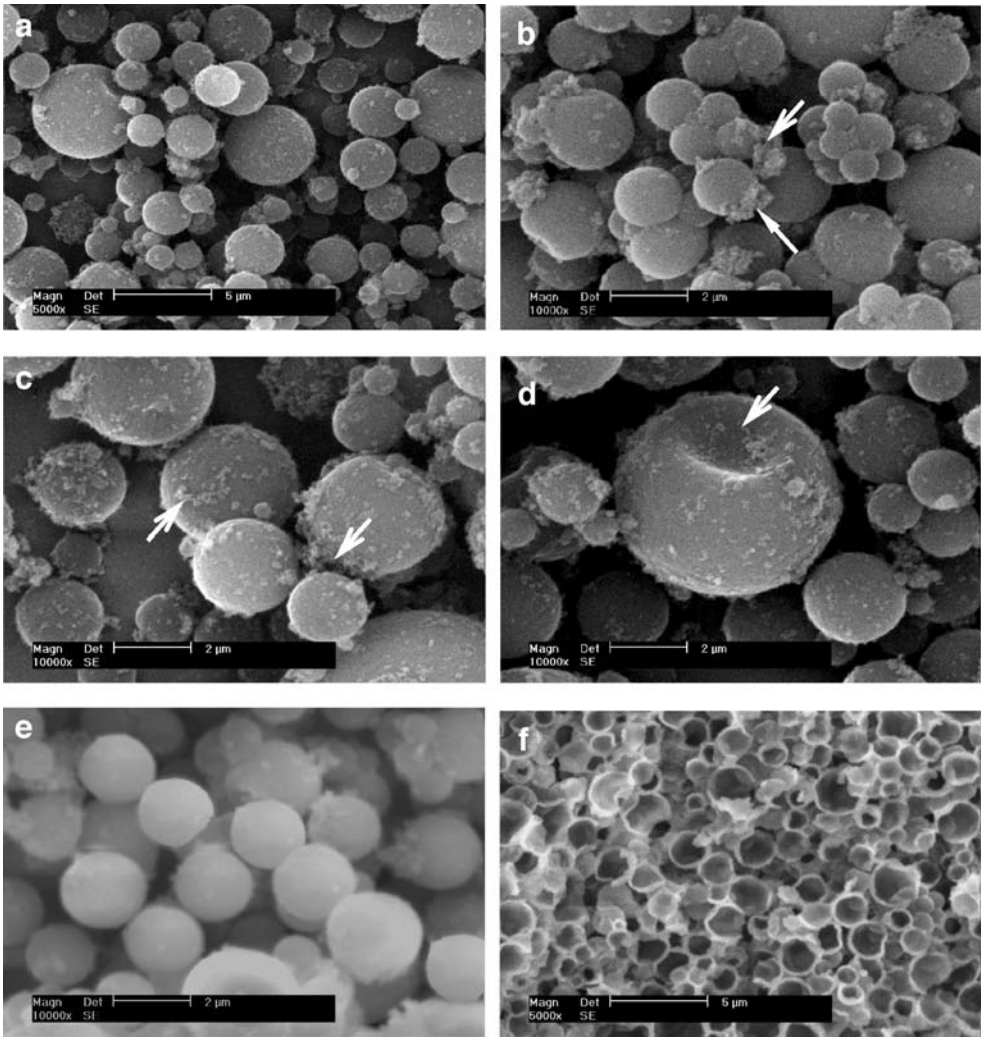

Fig. 3 SEM photographs of microcapsules dried in a vacuum oven at 40 °C for 24 h: **a**, **b** surface morphology of piled OSC microcapsules, **c**, **d** the rough surface morphology of OSC microcapsules, **e** surface morphology of piled TSC microcapsules, and **f** cross-section of TSC microcapsules

defects that OSC could not achieve a perfect coacervation on cores slowly and tightly in enough time under condition of mass shell material. Figure 3e reflects the surface morphology of piled microcapsules fabricated by TSC. It appears that nearly all these smooth microcapsules have a diameter of about 2 μm with regularly shaped globe. Moreover, not only is there nearly no concavoconvex and wrinkle embedded in shell surfaces, but also little polymer is pilling between piled microcapsules. These results reflect that the method of twice-dropping prepolymer has decreased the roughage through molecules regulation of the second-dropped polymer. At the same time, the flaws may be decreased by padding the second cross-linking on the previous coacervation.

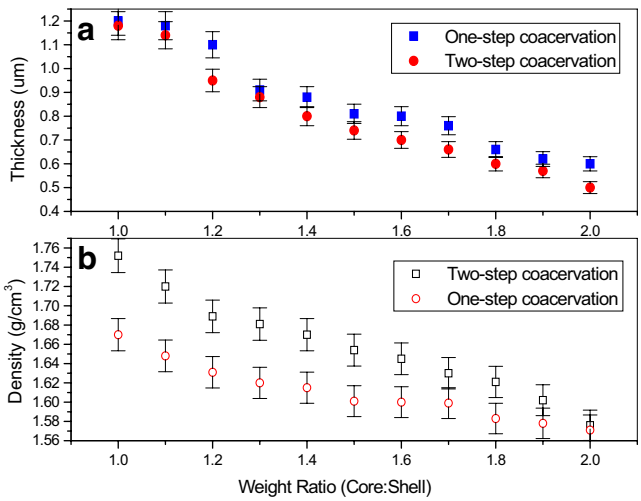

Fig. 4 The data of **a** shell thickness and **b** density fabricated by OSC and TSC with carious core and shell weight ratio

Density and thickness of shells

Density and thickness of shells are useful parameters reflecting the compactness of shells. Originally, the thickness data can be measured from cross-section SEM images as shown in Fig. 3f. In this study, a series of microcapsules were fabricated with various weight ratios of core (32 g) and shell materials from 1.0 to 2.0 (core: shell) by two kinds of coacervation methods to evaluate encapsulation

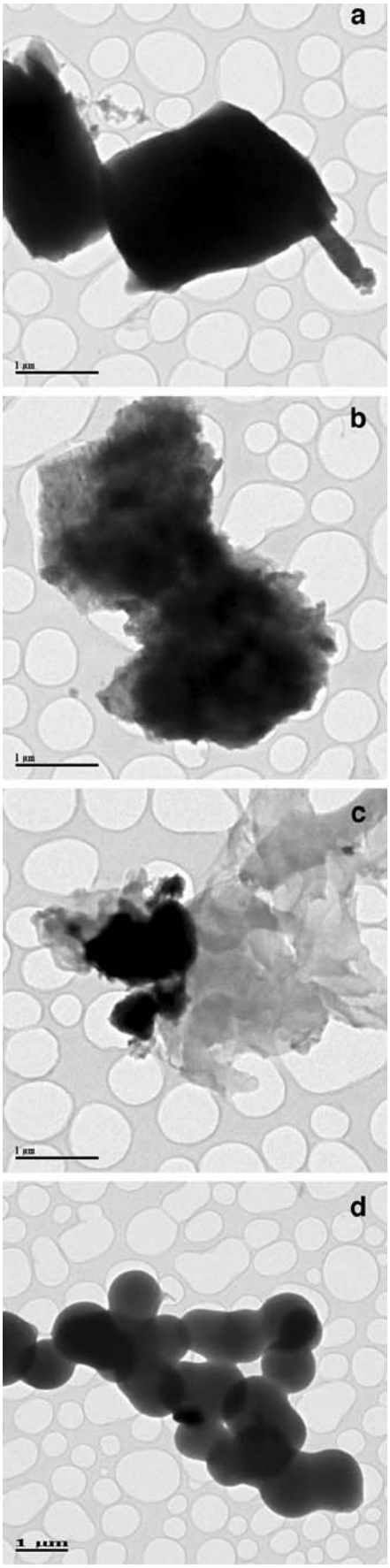

◀ **Fig. 5** TEM photographs of microcapsules in water: **a** OSC microcapsules in water for 30 min, **b** OSC microcapsules in water for 60 min, **c** OSC microcapsules in water for 90 min, and **d** TSC microcapsules in water for 90 min

effect. All the microcapsules had the same preparation materials and environmental conditions. At least 50 shells for each sample were measured and the average data were recorded by a MiVnt Image analyze system automatically.

The data in Fig. 4a show that the thickness of OSC and TSC shells are both decreased with the increasing of value of weight ratios. And at the same weight ratios, all the thickness of TSC shell is less than that of OSC. This may be attributed to two aspects. First, the TSC may decrease the structure defects, such as holes and caves. Second, this method of TSC allows the prepolymer to regulate their molecules on core material with enough reaction time for higher cross-linking density.

The data of density affected by various weight ratios are shown in Fig. 4b. At the same weight ratio of 1.0, the densities of OSC and TSC are 1.75 and 1.67 g/cm^3, respectively. With the increasing of weight ratio, both densities of OSC and TSC shells are decreased. And at the weight ratio point of 2.0, both kinks of microcapsules have a shell density of nearly 1.58 g/cm^3.

Shell stability in water

Usually, we may simply evaluate the compactability and stability of shell by observing the morphologic changes of shell in water during different times. This method will be helpful to understand the structures of shells. In our previous study, it had been found that the smaller microPCMs usually had the less stability in water [34]. Therefore, in this study, dried microcapsules with a diameter of 1 μm were applied for convenience to indicate the endurance of shells in water by means of TEM. Though observing the 1-μm microPCMs in water with the worst stability, we can conclude the practical effect of TSC. Subpanels a and b in Fig. 5 show the dried OSC microcapsules after being immersed in water for 60 and 120 min, respectively. It is found clearly that the microcapsules are not spherical in shape because of absorbing water. And after 150 min, the polymer shell peeled off from the core particles as shown in Fig. 5c. The peeled shells were in spreading state and the core material has been separated without covering. We show particular interest to Fig. 5d depicting the compact TSC microcapsules after being immersed in water for 150 min. Not only did the capsules still kept the original global sphere and size nearly without peeling and expansion, but the core material was also safely protected, avoiding releasing.

By referring back to Figs. 2 and 3, these above results are understandable in view of molecular structure of shells.

When hydrolyzed SMA molecules were absorbed at the interfaces of the oil particles, the molecules had directional arrangement with hydrophobic groups oriented into oil droplet. It was easy for water to permeate in the shells through cracks and capillary. The force of interface adhesion between core and shell would reduce due to the static electricity force decreased by the effect of water molecular. Then, OSC microcapsules were swelled and destroyed with time prolongation. Comparatively, shell of TSC microPCMs had less cracks and capillary, which also decreased the effect of water molecular.

Thermal stability of microcapsules

Figure 6 shows thermogravimetric (TGA/DTG) curves of microcapsules prepared during various coacervation times. The blue and red lines are curves of TGA and DTG curves, respectively. Both left and right axes are residual weight (wt%) of TGA curves and lost weight ratio of DTG curves. The microcapsules were decomposited with increasing temperature according to presenting residual weight (wt%). The curves may reflect thermal stability and structure of polymeric shell. Figure 6a shows that pure *n*-octadecane lost its weight at the beginning temperature of 137 °C and lost weight completely at 207 °C. To know the compactness of encapsulation effect, we compared TGA curves of the OSC microcapsules fabricated by prepolymer dropping rates of 0.5 (Fig. 6b) and 1.0 ml/min (Fig. 6c). Contrastively, both kinds of OSC microcapsules containing *n*-octadecane lost weight rapidly at the temperature of 100 °C. The loss of weight in the beginning may be some water and other molecule ingredients. And then the weight decreased sharply from 160 to 350 °C because of the cracking of shells. The weight loss speed of microcapsules was distinctly less than that of pure *n*-octadecane. Though it indicates that the OSC method can encapsulate the core material, we can draw a conclusion that the lower dropping speed of shell material has little effect on improving the shell compactness.

Figure 6d shows a TGA curve of the expected TSC microcapsules fabricated with dropping shell material speed of 0.5 ml/min. It loses weight between 200 and 400 °C. We also find that the beginning losing-weight temperature of TSC is higher than that of OSC, which indicates that the method of TSC has a better effect on protecting of core material.

Permeability of microPCMs

Release rate depends largely on the polymer structure of shells, which in turn is influenced by the conditions employed in preparation. A typical SEM morphology of microcapsules after releasing is shown in Fig. 7. The arrows indicate a broken shell structure formed during releasing process. Moreover, the weight ratio of core and shell will greatly affect the permeability. For example, we have discussed that penetrability of microPCMs with average diameter of 5 μm is lower than that of 1.5 μm. And their penetrability with a mass ratio of 1:1 (core/shell) is lower than that of 3:1 and 5:1 under the same core material emulsion speed [34]. Considering the above results, only one kind of microPCMs fabricated with a mass ratio of 1:1 and diameter of 5 μm were selected in this study to simplify the relationship between the fabrication process and the permeability. In addition, these shell structures were

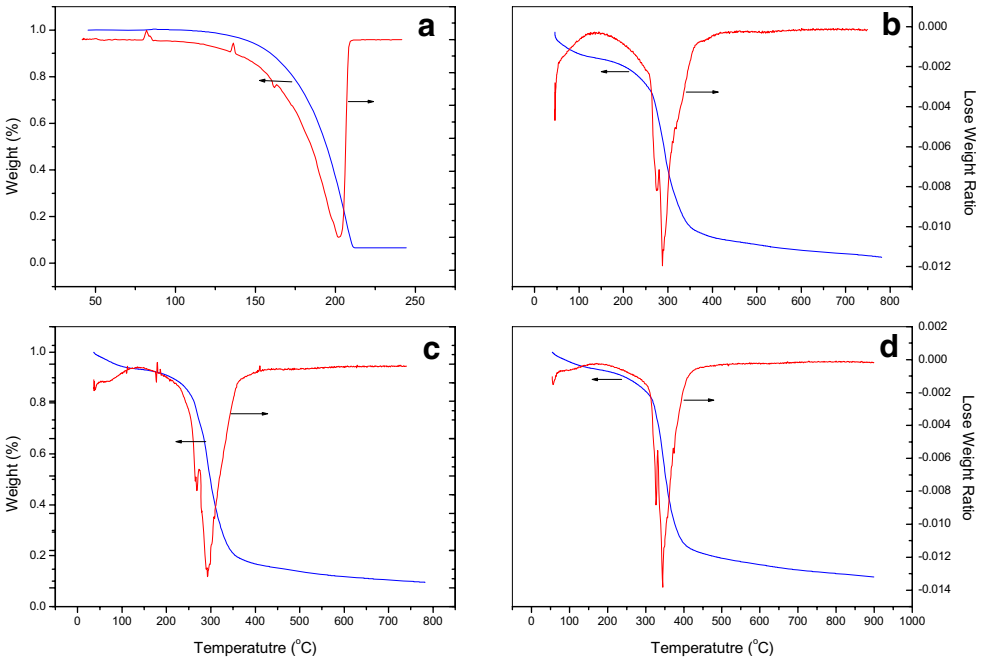

Fig. 6 TGA and DTG curves for **a** pure core material of *n*-octadecane, **b** OSC microcapsules fabricated by 0.5 ml/min dropping rate of the adding prepolymer, **c** OSC microcapsules fabricated by 1.0 ml/min dropping rate of the adding prepolymer, **d** TSC microcapsules fabricated by 0.5 ml/min dropping rate of the second adding prepolymer

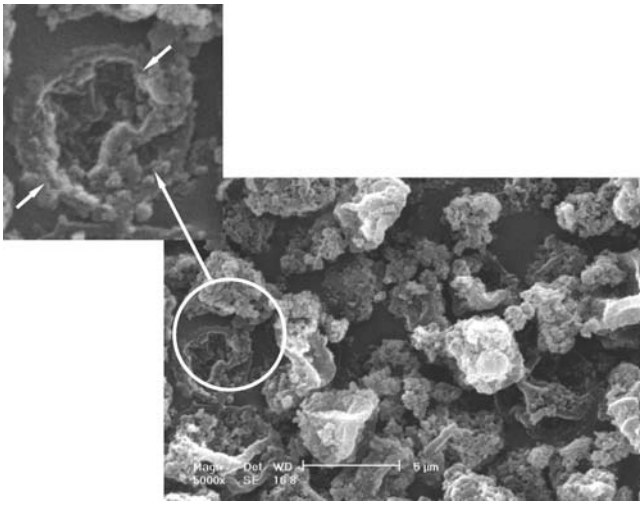

Fig. 7 A typical SEM morphology of broken microcapsules during releasing

fabricated by controlling the prepolymer dropping speeds at 0.5, 1.0, and 2.0 ml/min, respectively.

Figure 8 shows curves of relationship between the percentage residual weight (wt%) of core material in microcapsules and the time course of the transmittance. Five systems, coded as A–F, were measured in extraction solvent. Although the resultant microcapsules had been filtered and washed with water, there was still a little unencapsulated *n*-octadecane and other fabrication materials attaching on shells. Therefore, the initial transmittances in media are 98, 98, 98, 97, and 99%, which were nearly equal values. The rate of permeation of OSC microcapsules shell decreases in the order of system A, B, and C. It can be concluded that the shell prepolymer dropping rates affect

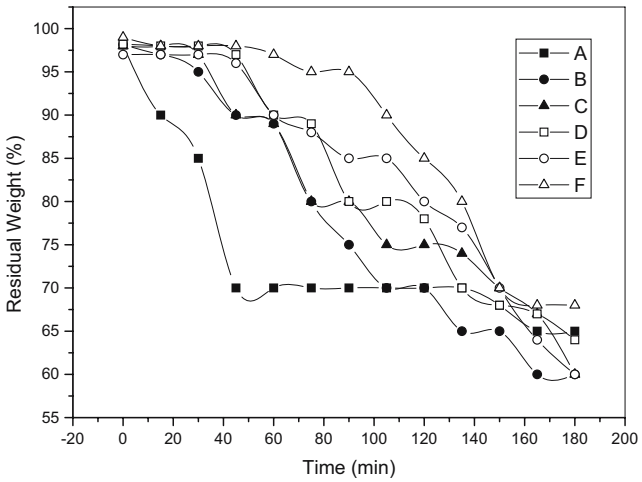

Fig. 8 Curves of the percentage residual weight (%) of core material in microcapsules in extraction solvent. The systems correspond to the conditions of coacervation methods and prepolymer dropping speed: *A* (*filled square*) OSC, 2.0 ml/min; *B* (*filled circle*) OSC, 1.0 ml/min; *C* (*filled triangle*) OSC, 0.5 ml/min; *D* (*open square*) TSC, 2.0 ml/min; *E* (*open circle*) TSC, 1.0 ml/min; and *F* (*open triangle*) TSC, 0.5 ml/min

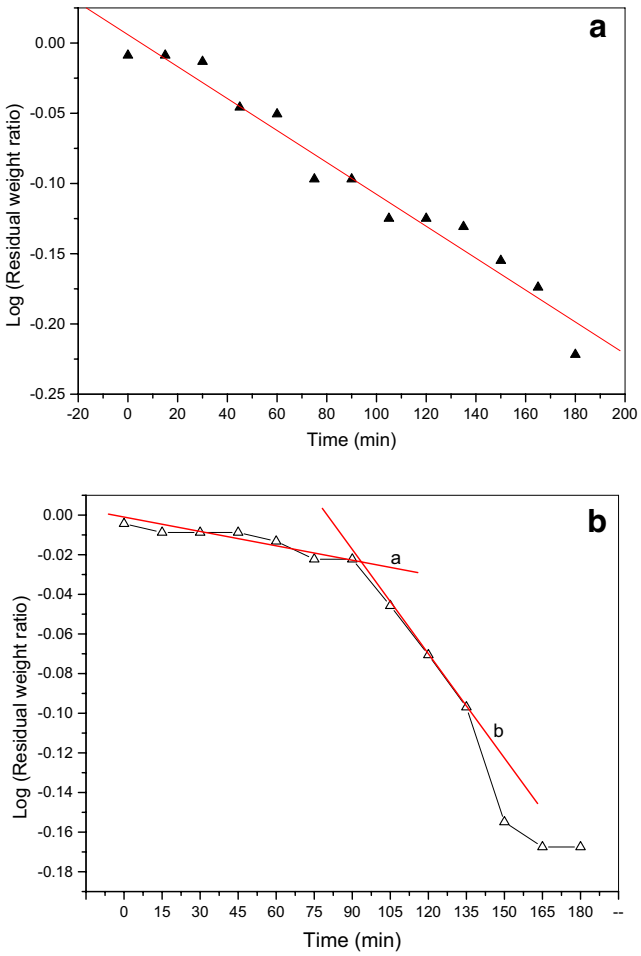

Fig. 9 The release curves of the OSC (**a**) and TSC (**b**) shells prepared by prepolymer material dropping rates of 0.5 ml/min

the penetrability directly. The total PCM permeated time from shells is just in 45 min of system A, compared to 90 min of system B and 125 min of system C. Especially, the release profile of system A is directly just in one step, but systems B and C have multisteps. Comparatively, the rates of permeation of TSC microcapsules decrease in the order of systems D, E, and F with multisteps. At the same time, the rates of permeation of TSC microPCMs are all lower than that of OSC ones even when fabricated at the same dropping rate. Moreover, the data in systems D, E, and F nearly do not change in the beginning of 50 min, and system F begins to change rapidly at the time of 90 min.

The reason for the above-mentioned phenomena may be attributed to two aspects. One is that the prepolymer concentration in solution determined by the dropping rate will affect the shells' formation speed. Under rapider dropping rate, the shell will be formed faster with enough shell material, which brings disfigurements, such as microcrack, microcavity, and capillary on shells. These disfigurements may lead the core material to penetrate with lower resistance. Contrarily, shells will form slowly under the

situation of low prepolymer concentration in solution. The prepolymer molecules will adhere on core particles compactly. On the other hand, the channels and disfigurements of penetration in shells are decreased by the twice-dropping fabrication method. The core material that penetrates the TSC shells needs longer distance and more time. Therefore, system F presents the best resistance of core material.

Permeability coefficient of the shell (k)

Generally, the kinetic theory of penetrability is determined by the structure and characteristic of shell. Fundamentally, by comparing the permeability coefficient of the shells (k), the minimum can be chosen fabricated by different preparation processes. Most of release properties observed in experiments have been analyzed by kinetic theories based on *Fick's law* with an assumption that the release rate is proportional to the concentration gradient of solutes [19, 20]. As each microcapsules system has different structure shell and core material, it is considered to be a complex system [21] and is required to employ different strict treatment to understand the release mechanism and to characterize such complex system clearly. In this study, we expect to get the compatible kinetic theory applied to the transfer of *n*-octadecane out of the TSC shell through the release curves of microcapsules in 20% (wt%) ethanol.

Figure 9 shows the release curves of systems C and F. It is a linear relationship between time and logarithmic residual weight of core of system C in Fig. 9a. Linear regression fit the first-order kinetic release theory [21],

$$2.303 \log q_{mc}/q_{\infty} = k_t \tag{3}$$

where q_{mc} is the residual weight of core material at time t; q_{∞} is the total weight of core material. The calculated value of k_1 (unit of k is s^{-1}) is

$$k_1 = -2.625 \times 10^{-3} \tag{4}$$

Figure 9b shows the release curve of system F with two decrease-linear steps (lines a and b) after curve regression. Lines a and b separate at the release time of 90 min and the release rate of the first step is lower that the of the second step. The TSC shell release curve of *n*-octadecane has a special release behavior, which reflects a complex shell structure. According to the calculation of Eq. 3, the value of k_2 and k_3 are

$$k_2 = -3.333 \times 10^{-4} \tag{5}$$

$$k_3 = -5.8333 \times 10^{-4} \tag{6}$$

By comparing the values of k_1, k_2, and k_3, it shows

$$k_2 > k_3 > k_1 \tag{7}$$

Conclusion

To increase the compact properties of MF shell microPCMs containing *n*-octadecane, a method of TSC encapsulation through an in situ polymerization was applied by dropping the shell material twice. All the evidences demonstrate that twice coacervations reduced the cracks on shells and increased the compactness of shells. Especially, we confirm that the shell resistance permeability is increased by TSC shell technology from the values of permeability coefficient k.

Acknowledgements The authors gratefully acknowledge Dr. Jinsheng Liang, Hebei University of Technology, for his valuable discussion.

References

1. Park SJ, Kim SH (2004) Preparation and characterization of biodegradable poly(L-lactide)/poly(ethylene glycol) microcapsules containing erythromycin by emulsion solvent evaporation technique. J Colloid Interface Sci 271:336–341
2. Zhang XX, Fan YF, Tao XM, Yick KL (2005) Crystallization and prevention of supercooling of microencapsulated *n*-alkanes. J Colloid Interface Sci 281:299–306
3. Yang R, Xu H, Zhang YP (2003) Preparation, physical property and thermal physical property of phase change microcapsule slurry and phase change emulsion. Sol Energy Mater Sol Cells 80:405–416
4. Mulligan JC, Colvin DP, Bryant YG (1996) Microencapsulated phase-change material suspensions for heat transfer in spacecraft thermal systems. J Spacecr Rockets 33:278–284
5. Han N, Zhang XX, Wang XC (2007) Fabrication, structures, and properties of acrylonitrile/methyl acrylate copolymers and copolymers containing microencapsulated phase change materials. J Appl Polym Sci 103:2776–2781
6. Cho JS, Kwon A, Cho CG (2002) Microencapsulation of octadecane as a phase-change material by interfacial polymerization in an emulsion system. Colloid Polym Sci 280:260–266
7. Holman Mark E (1999) Use of microencapsulated phase-change materials to enhance the thermal performance of apparel. Am Soc Mech Eng 44:235–239
8. Su JF, Wang LX, Ren L, Huang Z, Meng XW (2006) Preparation and characterization of polyurethane microcapsules containing *n*-octadecane with styrene-maleic anhydride as a surfactant by interfacial polycondensation. J Appl Polym Sci 102:4996–5006
9. Su JF, Wang LX, Ren L (2005) Preparation and characterization of double-MF shell microPCMs used in building materials. J Appl Polym Sci 97:1755–1762
10. MNA, Uddin MS, Zhu HJ (2000) Preparation and evaluation of a novel solar storage material: microencapsulated paraffin. Int J Sol Energy 20:227–238
11. Wang LY, Tsai PS, Yang YM (2006) Preparation of silica microspheres encapsulating phase-change material by sol–gel method in O/W emulsion. J Microencapsul 23:3–14
12. Hu XX, Zhang YP (2002) Novel insight and numerical analysis of convective heat transfer enhancement with microencapsulated

phase change material slurries: laminar flow in a circular tube with constant heat flux. Int J Heat Mass Transfer 45:3163–3172
13. Zhang XX, Tao XM,Yick KL, Wang XC (2004) Structure and thermal stability of microencapsulated phase-change materials. Colloid Polym Sci 282:330–336
14. Kim JW, Ko JY, Jun JB, Chang IS, Kang HH, Suh KD (2003) Multihollow polymer microcapsules by water-in-oil-in-water emulsion polymerization: morphological study and entrapment characteristics. Colloid Polym Sci 281:157–163
15. Hong K, Park S (1999) Preparation of polyurethane microcapsules with different soft segments and their characteristics. React Funct Polym 42:193–200
16. Zhang XX, Tao XM, Yick KL, Fan YF (2005) Expansion space and thermal stability of microencapsulated *n*-octadecane. J Appl Polym Sci 97:390–396
17. Mao ZW, Ma L, Gao CY, Shen JC (2005) Preformed microcapsules for loading and sustained release of ciprofloxacin hydrochloride. J Control Release 104:193–202
18. Shulki, Stover HDH (2002) Microcapsules from styrene-maleic anhydride copolymers: study of morphology and release behavior. J Membr Sci 209:433–444
19. Zhang XX, Wang XC, Tao XM, Yick KL (2005) Energy storage polymer/MicroPCMs blended chips and thermo-regulated fibers. J Mater Sci 40:3729–3734
20. Nihant N, Grandfils C, Jerome R, Teyssie P (1995) Microencapsulation by coacervation of poly(lactide-co-glycolide) IV. Effect of the processing parameters on coacervation and encapsulation. J Control Release 35:117–125
21. Makino K, Umetsu M, Goto Y, Kikuchi A, Sakurai Y, Okano T, Ohshima H (1999) Two-Layer structure of microcapsule membrane as predicted from electrophoretic studies. J Colloid Interface Sci 218:275–281
22. Jegat JL (2000) Taverdet, stirring speed influence study on the microencapsulation process and on the drug release from microcapsules. Polym Bull 44:345–351
23. Hong K, Park S (2000) Preparation of polyurea microcapsules containing ovalbumin. Mater Chem Phys 64:20–24
24. Hwang JS, Kim JN, Wee YJ, Jang HG, Kim SH, Ryu HW (2006) Factors affecting the characteristics of melamine resin microcapsules containing fragrant oils. Biotechnol Bioprocess Eng 11:391–395
25. Yadav SK, Khilar KC, Suresh AK (1997) Release rates from semi-crystalline polymer microcapsules formed by interfacial polycondensation. J Membr Sci 125:213–218
26. Zhang XX, Fan YF, Tao XM, Yick KL (2004) Fabrication and properties of microcapsules and nanocapsules containing *n*-octadecane. Mater Chem Phys 88:300–307
27. Shin Y, Yoo D, Son K (2005) Development of thermoregulating textile materials with microencapsulated phase change materials (PCM). II. Preparation and application of PCM microcapsules. J Appl Polym Sci 96:2005–2010
28. Laguecir, Frere Y, Danicher L, Burgard M (2002) Size effect of complexing microcapsules on copper ion extraction. Eur Polym J 38:977–981
29. Lebedeva, Kim BS, Vinogradova OI (2004) Mechanical properties of polyelectrolyte-filled multilayer microcapsules studied by atomic force and confocal microscopy. Langmuir 20:10685–10690
30. Kim YJ, Kim J, Lee SS, Kim WN, Kim MS (2006) Deformation and durability control of microcapsules for electrophoretic display system. Mol Crystals Liq Crystals 459:215–220
31. Hwang JS, Kim JN, Wee YJ, Yun JS, Jang HG, Kim SH, Ryu HW (2006) Preparation and characterization of melamine-formaidehyde resin microcapsules containing fragrant oil. Biotechnol Bioprocess Eng 11:332–336
32. Sun G, Zhang Z (2001) The mechanical properties of melamine–formaldehyde(M–F) microcapsules were studied using a micromanipulation technique. J Microencapsul 18:593–602
33. Rong Y, Chen HZ, Wei DC, Sun JZ, Wang M (2004) Microcapsules with compact membrane structure from gelatin and styrene-maleic anhydride copolymer by complex coacervation. Colloids Surf A Physicochem Eng Asp 242:17–20
34. Wang LX, Su JF, Ren L (2005) Preparation of thermal energy storage microcapsules by phase change. Polym Mater Sci Eng 21:276–279